18th World IMACS / MODSIM Congress, Cairns, Australia 13-17 July 2009
http://mssanz.org.au/modsim09

A Model for Steady-State Oil Transport and Saturation in a Mist Filter

D. Kampa[1], J. Meyer[1], B. Mullins[2] and G. Kasper[1]

[1]*Institut für Mechanische Verfahrenstechnik und Mechanik, Universität Karlsruhe (TH), 76128 Karlsruhe, Germany*
[2]*Centre of Excellence in Cleaner Production, Curtin University of Technology, Perth, WA 6845, Australia*
Email: daniel.kampa@mvm.uni-karlsruhe.de

Abstract: This work details the development and sensitivity analysis of a model to predict the spatial saturation profile in oil mist filters in the air flow direction.

Oil-mists are generated by many industrial processes, including engine crankcase ventilation and generation of compressed air by oil lubricated compressors. It is necessary to remove these mists to avoid problems further downstream or to meet health and safety regulations. The most common method for removing such particles from an air stream is the use of fibrous filters. Such filters operate for almost their entire life in a steady state, in which the saturation becomes independent of time for a constant set of operating conditions. However, in this steady state, the saturation varies spatially within the filter, due to the following effects (Figure 1):

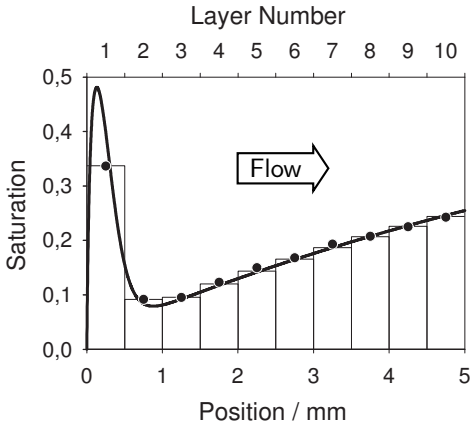

Figure 1: The experimental saturation profile (circles), measured by determining the average layer saturation of a filter consisting of 10 layers (filtration velocity 0.3 m s^{-1}, loading rate 20 g h^{-1} m^{-2}, layer efficiency > 0.95) is well represented by the model (line and resulting average layer saturation as bar chart).

- When the oil droplets from the aerosol are captured by the fibres, the saturation rises.
- Oil within the filter drains due to gravity, hence the saturation decreases.
- Since the oil cannot flow out of the filter at the rear freely, i.e. without forming larger drops, a barrier exists. In front of this barrier, the oil is "piled up" (static saturation) with a linear slope due to flow forces.
- At higher saturation, the flow velocity and hence the flow forces driving the oil out increase. This explains the decline of the slope on the downstream side of the filter.

These effects were modeled using known physical relationships. The modelled saturation profile agrees well with the experiment, once the model was fitted to the data (Figure 1). Based on the model, a sensitivity analysis was performed, to show the effect of each parameter on the saturation profile.

Keywords: *mist filtration, coalescence filter, saturation profile, analytical model*

1 INTRODUCTION

Oil-mists are generated by many industrial processes, including engine crankcase ventilation and generation of compressed air by oil lubricated compressors. It is necessary to remove these mists to avoid problems further downstream or to meet health and safety regulations. Mist droplets are deposited on the fibres due to diffusion, interception or inertial impaction (Brown, 1993). With more and more droplets being captured by a fibre, they coalesce into larger drops (Yarin et al., 2006). Their transport within the filter is determined by gravitational and flow forces. When a large drop flows along a (wetting) fibre, it leaves a film (Agranovski and Braddok, 1998). Such films, as well as large drops can join together and form liquid bridges at fibre intersections and between fibres (Liew and Conder, 1985; Mullins et al., 2004), which remain equalised under capillary forces. Thereafter a steady state is reached, where oil accumulation and drainage rates balance out (Contal et al., 2004). Filters operate in such a steady state for almost their entire life. A kinetic model was developed to describe the spatial distribution of oil within the filter. The model is based on the balance between oil accumulation and transport rates within an infinitesimal layer.

2 MODEL DEVELOPMENT

The oil saturation S of the filter is a measure of the amount of liquid within the filter. It is defined as the fraction of filled void space,

$$S = \frac{V_{\text{liquid}}}{V_{\text{filter}} - V_{\text{fibres}}}$$

where V_{filter} is the total volume of the filter, V_{fibres} the volume of the fibres and V_{liquid} the volume of the oil inside the filter. By definition, the saturation can vary between zero and one. In this section, the physical effects and their influence on the saturation $S(x)$, where x is the coordinate in the flow direction, are described phenomenologically.

2.1 Deposition of droplets and transport in the flow direction

At the upstream side of the filter, at $x = 0$, there are no fibres and hence all the oil mass is located in the aerosol yielding a saturation of $S(0) = 0$ (Figure 2). As soon as the oil mist enters the filter, droplets are captured by the fibres and the collected oil is transported in the direction of the gas flow. While the oil concentration in the aerosol decreases, the saturation increases towards the rear of the filter. After some filter length, hardly any droplets remain in the aerosol, and consequently, the saturation levels off. By flow forces, all oil within the filter is transported to the rear of the filter, where it finally spills out. Since the oil inside of the filter, described by the saturation (light and medium red, Figure 2), is transported oil, it is called dynamic saturation.

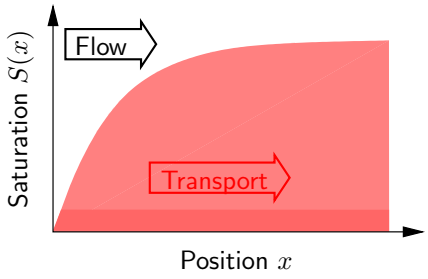

Figure 2: Saturation profile considering droplet deposition and transport in the flow direction.

2.2 Internal drainage

Neglecting flow forces, oil drains due to gravity from a completely saturated filter according the classical Washburn-equation (Washburn, 1921). Similar drainage behaviour is assumed for oil in the filter, when air passes through it. As saturation increases, the drainage rate increases correspondingly. The effect on the saturation profile from Section 2.1 (Figure 2) is, that, as soon as oil is available, it will drain off, hence the oil being transported to the rear of the filter decreases and so does the saturation (Figure 3). However, the dynamic saturation does not approach zero, since some residual oil is kept by capillary forces (medium red, Figures 2-4).

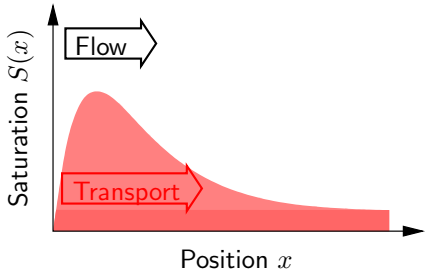

Figure 3: Saturation profile considering droplet deposition, transport in the flow direction and internal drainage.

2.3 Rear barrier

It was observed, that oil does not only drain inside of the filter medium, but also at its rear. This rear drainage is performed by individual large drops flowing downwards at the rear of the filter. The generation of these large drops from the coalesced drops along the fibres requires some energy and some amount of oil resulting in a barrier for the transported oil located at the rear. In front of this barrier, the transported oil piles up, yielding the static saturation. If the drag force does not depend on the position, the slope of the static saturation is linear.

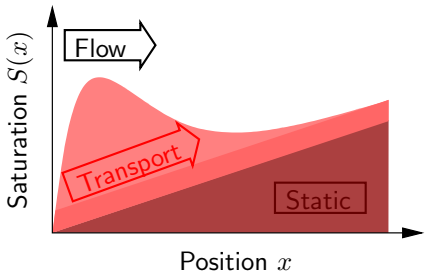

Figure 4: Saturation profile considering droplet deposition, transport in the flow direction, internal drainage and the static saturation at rear due to the barrier needed for formation of the rear drainage.

This static saturation does not influence the internal drainage. However, it adds to the dynamic saturation (Figure 4). The resulting saturation profile resembles the well-known U-shape of saturation profile.

2.4 Flow velocity dependent saturation

Thus far, the influence of saturation on flow velocity and vice versa was not considered. However, a high saturation, i.e. a low void space at a given position, results in a high local flow velocity. This incurs a large drag force on the oil drops within the filter, which passes them downstream more quickly and finally results in a lower saturation. A consequence of this effect is that the slope of the static saturation declines towards the downstream side of the filter, where higher saturations appear.

2.5 Model formulation

To model the saturation profile, a mass balance between oil accumulation and transport rates within an infinitesimal layer was drawn. It yields a first order non-linear differential equation,

$$\frac{d}{dx}\underbrace{\Big(S(x)-S_{\mathrm{stat}}\big(x,S(x)\big)\Big)}_{\text{dynamic saturation}} \propto \big(1-S(x)\big)^2\Bigg[\underbrace{\int \mathrm{d}d_{\mathrm{p}}\, f(d_{\mathrm{p}})\mathrm{e}^{g(d_{\mathrm{p}})x}}_{\text{particle collection}} - \underbrace{d\left(1-\frac{c}{S(x)-S_{\mathrm{stat}}\big(x,S(x)\big)}\right)}_{\text{drainage}}\Bigg], \tag{1}$$

with the static saturation $S_{\mathrm{stat}}\big(x,S(x)\big) \propto sx\big(1-S(x)\big)^2$, where s is the static potential. The particle collection term originates from the filter theory (Brown, 1993) and accounts for the different sizes d_{p} of generated mist droplets. $f(d_{\mathrm{p}})$ and $g(d_{\mathrm{p}})$ depend on the particle collection efficiency and $f(d_{\mathrm{p}})$ is proportional to the oil concentration. The drainage term, depending on the drainage rate d and a drainage specific constant c, results from the classical Washburn-equation (Washburn, 1921). The change in dynamic saturation, i.e. in transported oil (left hand side of (1)), is caused by particle collection and by drainage (right hand side of (1)).

The differential equation (1) was solved numerically in Matlab using the explicit Runge-Kutta (4,5) algorithm (solver *ode45*).

3 COMPARISSON TO EXPERIMENT

To measure a saturation profile, filters consisting of ten layers of oleophobic glass fibre media (layer efficiency > 0.95) were loaded with oil mist (loading rate 20 g h^{-1} m^{-2}) which was generated by an atomizer and was flowing against the filter with 0.3 m s^{-1}. After the steady state was reached, the flow was stopped, the filter disassembled and the saturation of each layer was determined gravimetrically.

The shape of the measured saturation profile (circles, Figure 1) is well represented by the model (line and resulting average layer saturation as bar chart, Figure 1). Since the parameters c, d and s can not be measured directly as yet, they were fitted to the data.

4 SENSITIVITY ANALYSIS

To observe the influence of several model parameters on the saturation profile, each parameter was varied, with all the other parameters kept constant. The starting point of each parameter variation is always the experimentally determined saturation profile (Figure 1, black lines in Figures 5-8).

4.1 Internal drainage

At high drainage rates, the oil is drained immediately, once aerosol droplets have been captured by the fibres. So the initial peak is smaller than for the measured saturation (black line, Figure 5). The lower the drainage rate, the larger the filter length where significant drainage occurs. After all transported oil being drained, the saturation at the upstream end of the filter converges to the static saturation profile. At very low drainage rates, the transported oil cannot be drained within the whole filter length. The consequence is, that the saturation at the very end of the filter reaches a higher value than the potential barrier, due to additional dynamic saturation.

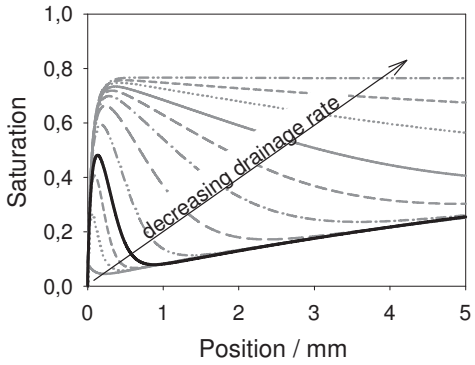

Figure 5: Saturation profiles for different drainage rates compared to the experimental observation (black, see also Figure 1).

4.2 Particle collection efficiency

The ability of a filter to capture oil droplets from the aerosol is described by the filter efficiency. Efficiencies larger than for the measured saturation (black line, Figure 6) lead to an oil deposition located further towards the front of the filter and more focused on a specific region (solid grey line, Figure 6). Since the internal drainage increases with increasing saturation, significantly more oil drains in the front layers of the filter in contrast to the measured filter. Efficiencies smaller than for the measured filter yield a more equally distributed saturation in the upstream part of the filter. This is due to aerosol deposition taking place in a larger region of the filter at lower saturation. The low saturation results in a low drainage rate and hence more oil is pushed forward in the flow direction.

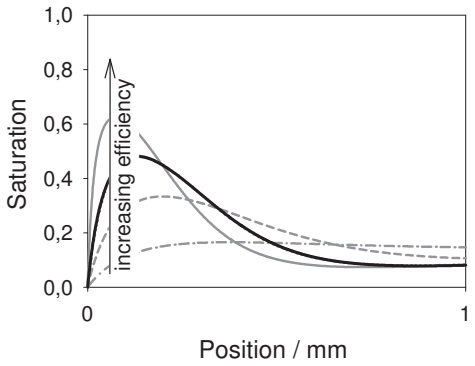

Figure 6: Saturation profiles for different efficiencies rates compared to the experimental observation (black, see also Figure 1).

4.3 Static saturation

For decreasing static potential, the slope of the saturation profile at the downstream side of the filter decreases until it approaches zero (Figure 7). In this case, however, the saturation is still larger than zero due to oil held up by capillary forces, which cannot be pushed downstream to the rear of the filter (Section 2.2). For increasing static potential i.e. potential

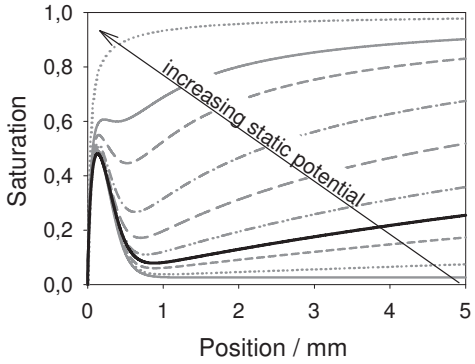

Figure 7: Saturation profiles for different static potentials compared to the experimental observation (black, see also Figure 1).

barrier at the rear, the slope of the saturation profile increases. For saturations approaching one, the slope declines due to flow velocity dependent saturation effects (Section 2.4).

4.4 Loading rate

For increasing oil concentration in the aerosol, the initial increase due to deposition reaches a higher peak (Figure 8). For very large oil accumulation rates, the medium is unable to drain all accumulated oil, which is consequently pushed downstream.

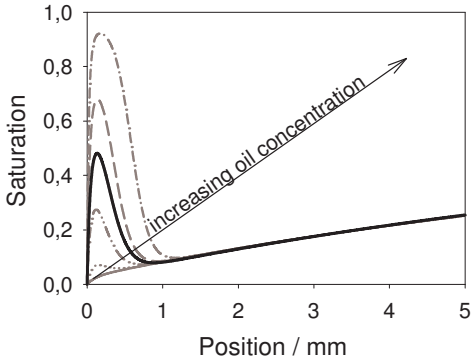

Figure 8: Saturation profiles for different oil concentrations compared to the experimental observation (black, see also Figure 1).

5 CONCLUSIONS AND OUTLOOK

A model for the saturation profile of a mist filter, which considers particle collection, internal drainage and the static saturation due to a rear face barrier and which accounts for the dependence of the saturation on the flow was developed. Based on the resulting differential equation a parameter variation, to show the influence of each model parameter was performed.

Industrial applications of oil mist filters aim to maximize filter efficiency and to minimise pressure drop across the filter. So far, the change in efficiency with filter loading has not been considered, since the effect on the saturation is small. For the saturated media, the efficiency can be calculated by either assuming that the accumulated oil increases the average fibre diameter (Frising et al., 2005) or that the drops on the fibres lead to a decrease in fibre length available for collection (Raynor and Leith, 2000). To calculate the pressure drop from the saturation, several models are available in the literature (Frising et al., 2005; Andan et al., 2008). After the media specific parameters have been determined experimentally, the model can be used to develop a software based filter optimisation tool.

ACKNOWLEDGMENTS

The authors acknowledge the German Research Foundation (DFG, grant number MU 2652/2-1) and MANN + HUMMEL for funding assistance.

REFERENCES

Agranowski, I.E. and Braddok, R.D. (1998), Filtration of liquid aerosols on wettable fibrous filters. *AIChE Journal*, 44, 2775-2783.

Andan, S., Hariharan, S.I. and Chase, G.G. (2008), Continuum model evaluation of the effect of saturation on coalescence filtration. *Separation Science and Technology*, 43, 1955-1973.

Brown, R.C. (1993), Air Filtration. *Pergamon Press, New York*.

Contal, P., Simao, J., Thomas, D., Frising, T., Callé, S., Appert-Collin, J.C. and Bémer, D. (2004) Clogging of fibre filters by submicron droplets. Phenomena and influence of operating conditions, *Aerosol Science*, 35, 263-278.

Frising, T, Thomas, D., Bémer, D. and Contal, P. (2005) Clogging of fibrous filters by liquid aerosol particles: Experimental and phenomenological modelling study. *Chemical Engineering Science*, 60, 2751-2762.

Liew, T.P. and Conder, J.R. (1985), Fine mist filtration by wet filters - I. Liquid saturation and flow resistance of fibrous filters. *Journal of Aerosol Science*, 16, 497-509.

Mullins, B.J., Agranovski, I.E., Braddok, R.D. and Ho, C.M. (2004), Effect of fiber orientation on fiber wetting processes. *Journal of Colloid and Interface Science*, 269, 449-458.

Raynor, P.C. and Leith, D. (2000) The influence of accumulated liquid on fibrous filter performance. *Journal of Aerosol Science*, 31, 19-34.

Washburn, E.W. (1921), The dynamics of capillary flow. *Physical Review*, 17, 273-283.

Yarin, A.L., Chase, G.G., Liu, W. Doiphode, S.V. and Reneker (2006), D.H., Liquid drop growth on a fibre. *AIChE Journal*, 52, 217-227.